Gas hydrate and methane plumes at Hydrate Ridge.

Kristen Schmidt, College of William and Mary
Mentors: Peter Brewer and Edward Peltzer
Summer 2004

ABSTRACT

Multiple measurements of free gas composition from active gas vents on Hydrate Ridge, Cascadia accretionary prism, were accomplished in 2000 and 2004 using the Monterey Bay Aquarium Research Institute vessel, R/V Western Flyer, and ROV Tiburon. An HP gas chromatograph was used for sample analysis, as well as an *in situ* laser Raman spectroscopy system developed at MBARI. Results indicate the composition of free gas is predominantly methane, with trace amounts of higher hydrocarbons (ethane through iso-pentane). This lends support for the kinetic mechanism theory that states free gas exists within the hydrate stability zone encased in hydrate lined reservoirs and conduits and isolated from the surrounding sediment matrix. The gases found also indicate that Hydrate Ridge is a mixed hydrate of Structure I, II, and H hydrates. Ratios calculated from the constituent gas concentrations signify the free gas as being mainly biogenically derived through bacterial methanogenesis, mixed with very small amounts of gas of thermogenic origin.

1. INTRODUCTION

1.1 BACKGROUND

Oceanic clathrates, natural gas hydrate deposits, are found generally in passive margins, active regions of plate collision, and marginal basins (Kvenvolden, 1993). They have become a subject widely focused on in research because of their potential importance as: (1) a future energy source (Kvenvolden, 1988), (2) a detrimental contribution to global warming (Dickens et al., 1995), and (3) a geologic threat in the case of massive oceanic landslides (Paull et al., 1996).

Gas hydrates, an ice-like crystalline compound, form when H_2O creates a rigid cage around a "guest" gas molecule, and are stable at low temperatures and high pressures. The gas can be CO_2, H_2S, methane, or higher hydrocarbons, and either biogenically derived or thermogenically produced. Hydrates of three distinct structures, or a mix of the three, are possible (Figure 1). Structure I contains a body-centered cubic lattice, and is mostly comprised of biogenic methane; Structure II forms a diamond lattice using methane through iso-butane ($C_1 \rightarrow i\text{-}C_4$); and Structure H is made out of a hexagonal lattice including methane through iso-pentane ($C_1 \rightarrow i\text{-}C_5$) (Sassen et al., 2004).
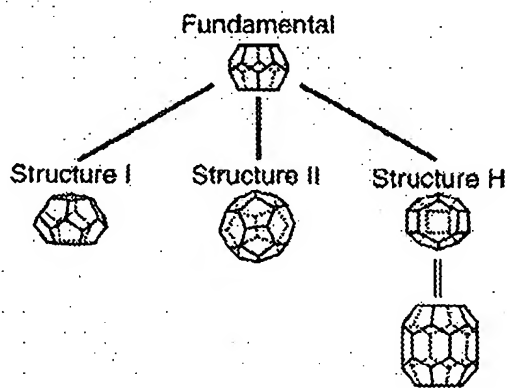

Figure 1: Possible Structures of gas hydrates. (Sloan, 1998)

More than 99% of deep ocean hydrates consists of methane hydrate. If the physico-chemical conditions are satisfied, hydrate will form; however, hydrate is less dense than the surrounding seawater and will float toward the surface until it decomposes. Thus, natural oceanic hydrates are found in the sediment which traps them

in the seafloor (Dillion & Max, 2000). A typical gas hydrate stability profile is illustrated in Figure 2. Below the seafloor gas hydrate exists, and continues to a depth until the temperature of the sediment rises above the phase boundary parameter. Below this depth, the natural gas in the hydrates is in the free gas state.
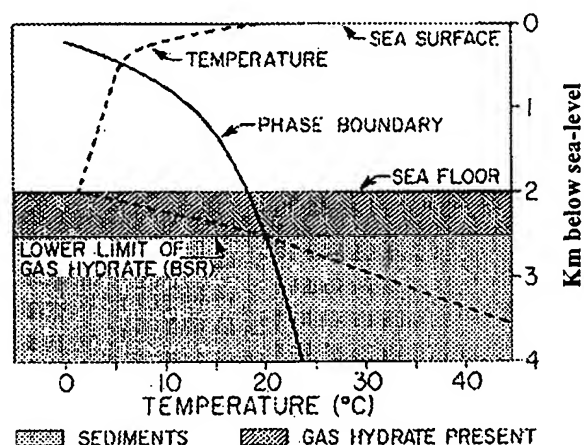

Figure 2: Gas hydrate stability profile. (Dillon & Max, 2000)

Gas hydrates vary not only in chemical properties, but also in physical properties, where there are characteristic end-members in terms of ocean hydrate systems. Blake Ridge, located to the southwest of the South Carolina coastline, is in a somewhat steady-state characterized by diffuse pore water flow driving the movement of gas, and hydrate that mostly exists in sediment pore spaces. In contrast, Hydrate Ridge, where this study is focused, illustrates episodic and vigorous free gas ebullition, with massive gas hydrates hosted in the sediment column (Tryon et al., 2002). This study presents analysis of free gas sampled at this end-member system from two different years, and compares that data with results from an *in situ* laser Raman spectrometer developed recently at the Monterey Bay Aquarium Research Institute. Sampling and measurements were made in 2000 and 2004 using the R/V *Western Flyer* and the ROV (Remotely Operated Vehicle) *Tiburon*.

1.2 GEOLOGIC SETTING

Hydrate Ridge (HR) is an accretionary wedge located 90km off the coast of Oregon in the tectonically active Cascadia subduction zone created by the oblique subduction of the Juan de Fuca Plate beneath the North American Plate (MacKay et al.,

3

1992). HR is 20km long and 15km wide, and with a northern summit at ~600mbsf, and a southern summit at ~800mbsf (Torres et al., 2002; see Figure 3).
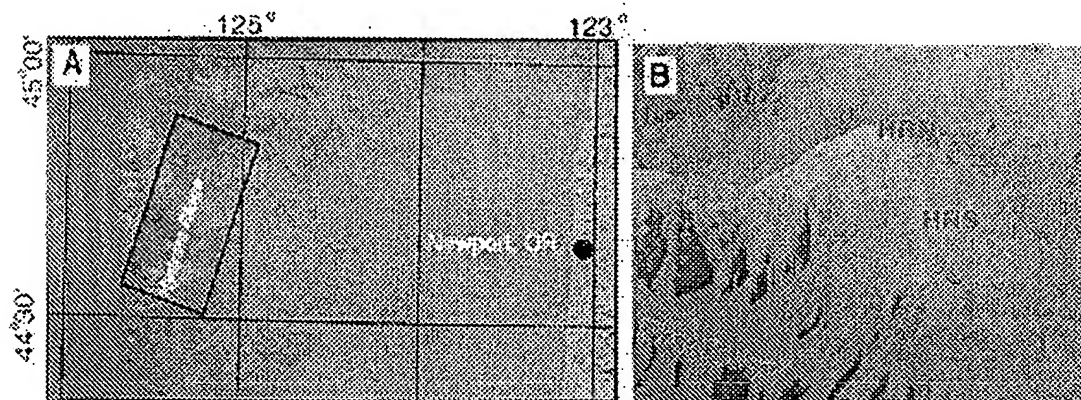

Figure 3: A. The location of Hydrate Ridge around 90km offshore. B. Bathymetric image of Hydrate Ridge shows the northern (600mbsf) and southern (800mbsf) summits.

Both summits have been observed to have methane bubble plumes that form from free gas expulsion from the sediment below (Torres et al., 2002), however Southern Hydrate Ridge is considered to be a younger vigorous venting site due to the absence of authigenic carbonate deposits (Trehu et al., 1999). The fact that free gas exists in the gas hydrate stability zone is of significance, where two different mechanisms have been proposed to account for this. Milkov et al. (2004) suggests that hydrate formation from free gas and water continually excludes dissolved ions causing the salinity of the surrounding pore water to increase. Increasing salinity then establishes equilibrium between gas hydrate, free gas, and brine, allowing any excess gas to enter the gas hydrate stability zone as free gas. In opposition, the kinetic mechanism theorizes that free gas enters the hydrate stability zone through conduits and chambers that become lined by gas hydrate as they form. These free gas spaces become isolated from the adjacent sediments and pore waters, excluding the water necessary to form additional hydrate (Suess et al., 1999; Trehu et al., 1999). It is currently unclear which means of gas ebullition is utilized, or if the two contribute in concert.

2. MATERIALS AND METHODS

2.1 FREE GAS SAMPLING

Gas samples were collected at Hydrate Ridge using a gas collection funnel that was positioned and maneuvered by the ROV Tiburon's robotic arm. The gas sampling device consists of a polycarbonate funnel, 10 inches deep, attached to a polycarbonate tube mounted through an acrylic base plate (Figure 4). The funnel was placed over a site of an active gas venting plume. In 2000, it was observed that gas collected in the funnel formed a hydrate skin, interfering with proper sampling of the gas at the site depth, and potentially altering the composition of the remaining free gas. In response, a 300 Watt, 240 Volt, fast-heat, 10 in. heater was incorporated into the device. The heater was encased in an oil filled copper tube, which served as a pressure housing that permitted efficient heat transfer to the sampling device, and connected to the ROV by an oil filled cable. The heater extends well into the funnel and was successful in decomposing the hydrate formed by the free gas.

Figure 4: The MBARI Free Gas Sampler with partial hydrate formed from free gas collection.

Mounted on the acrylic plate are three 150ml stainless steel cylinders rated to 1800 internal psi. The cylinders were cleaned with organic solvents (acetone and methylene chloride), assembled, pressurized with Hydrogen gas (~930 psig), and submerged in water to check for potential leaks. The cylinders were stored pressurized and evacuated immediately prior to the dive. Following gas collection in the sample funnel, an actuator triggered the sample to flow through a 5-way Swagelok valve, a check valve and into one

of the cylinders. Post-dive, the gas samples were split by expanding them into a cylinder of equal volume, and then stored for post-cruise analysis.

2.2 GAS SAMPLE ANALYSIS

The gas samples were analyzed for the relative concentrations of hydrocarbons (C_1-C_6), CO_2, and air, using an HP 5890 Series II Gas Chromatograph (GC). The presence of H_2S gas was detected by olfactory means. The GC uses two methods of detection: a flame ionization detector (FID) and a thermal conductivity detector (TCD). The FID determines the concentrations of the combustible hydrocarbons, is very selective, and has a large linear range. The TCD detects the change in thermal conductivity by comparing the thermal conductivity of the carrier gas (helium) with that of the He diluted gas sample. The TCD has a much lower sensitivity than the FID, but is necessary to obtain the concentration levels of the non-combustible CO_2 and air.

Each sample was injected into a 95.2µL loop, and the ambient temperature and pressure were recorded. The samples were then reanalyzed using a 1.002mL sample loop to increase the detection limit for gases present in very low concentration. A standard gas mixture was also analyzed at both the beginning and end of the sample set for calibration. The data were integrated using HP ChemStation software.

To determine the concentrations of the gases in each sample, peak area analysis was used in combination with response factors calculated from the standard gas mix. The calculations for the response factors and concentrations are as follows:

$$R = \frac{A_{std}}{C_{std} * 10^4} = \left(\frac{area}{ppm}\right)$$

$$C = \frac{A_{smp}}{R * 10^4} = (\%)$$

Where R is the response factor, A_{std} is the peak area of the gas in the standard at STP, C_{std} is the concentration of gas in the standard (%), A_{smp} is the peak area of the gas in the sample at STP, and C is the concentration of gas in the sample as a percent of the total.

2.3 LASER RAMAN SPECTROSCOPY

The ROV Tiburon was also used to make in situ analyses using the MBARI designed DORISS (Deep-Ocean Raman *In Situ* Spectrometer) apparatus (Brewer et al., 2004; Pasteris et al., 2004). DORISS uses a 532nm wavelength (green) laser with an immersion optic that penetrates about 2cm into the gas cube (Figure 5). The cube measures (11"L x 4"W x 4"H), has PVC sides, a clear acrylic front, and is outfitted with the same heater as the gas sampling device to prevent hydrate formation. Once the cube filled with a sufficient amount of gas, the lights on the ROV were powered down so as to not interfere with the acquisition of spectra (Figure 6). Each spectrum is an average of 10 accumulations of 30 second exposures.
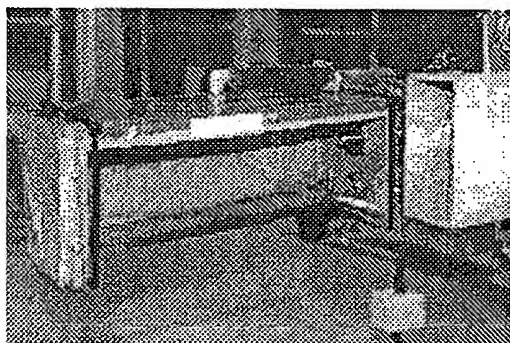

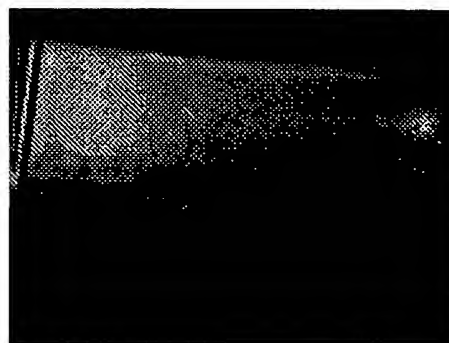**Figure 5: The MBARI gas cube on DORISS with immersion optic and heater.**

Figure 6: An Acquistion of Raman spectrum. Hydrate is on the inside of the gas cube window.

3. RESULTS

3.1 FREE GAS SAMPLES

Active venting of methane bubbles was observed on two different occasions (2000 and 2004), at the southern summit of Hydrate Ridge with three different sites sampled. Two samples were taken from Flag Pit in 2000, HRW12 and HRW13. Each was analyzed in duplicate; thus, HR2000A and HR2000B are averaged concentration data sets. Two sites were sampled in 2004: Pinkie Vent North (identified with a large plastic pink flamingo) and Marker 17, yielding a total of 6 samples (Table 1).

Table 1: Sample sites on Hydrate Ridge.

Site	Sample	Latitude	Longitute
Flag Pit	HR2000A	44.57077	-125.14850
	HR2000B	44.57077	-125.14850
Pinkie	T704RedA	44.57055	-125.14830
Vent	T704BlueA	44.57055	-125.14830
North	T704BlackA	44.57055	-125.14830
	T705BlackA	44.57062	-125.14825
Marker	T705RedA	44.57003	-125.14670
17	T705BlueA	44.57003	-125.14670

The samples displayed a relatively consistent composition, chiefly comprised of methane gas (C_1; 95.3% to 99.4%), with much smaller percentages of the higher hydrocarbons ethane, propane, iso-butane, normal butane, and iso-pentane (C_2-iC_5; <0.2%). The concentration level of each component is largely consistent within a sample site. Although the GC is able to detect normal pentane at trace levels (C_5), it was not detected in any sample. The absence of significant odor indicated that the samples did not contain H_2S gas. The amount of air and CO_2 was also relatively consistent at each sample site (Table 2).

Table 2: Gas chromatographic analysis results of Hydrate Ridge samples.

Sample	Air % (N$_2$)	CO$_2$ %	C$_1$ %	C$_2$ %	C$_3$ %	i-C$_4$ %	C$_4$ %	i-C$_5$ %	Ratio C$_1$/(C$_2$+C$_3$)	Ratio C$_2$/C$_3$	Ratio i-C$_4$/C$_4$	Total %
HR2000A	1.760	0.132	95.3	0.080	0.027	0.008	0.010	0.006	899	3.00	0.842	97.3
HR2000B	1.085	0.136	98.8	0.082	0.027	0.008	0.010	0.005	906	3.04	0.842	100.1
T704Red	0.897	0.175	97.1	0.100	0.038	0.014	0.018	0.012	704	2.63	0.778	98.4
T704Blue	0.590	0.166	98.4	0.099	0.025	0.007	0.009	0.005	793	3.96	0.778	99.3
T704Black	0.571	0.175	99.1	0.098	0.025	0.007	0.009	0.005	806	3.92	0.778	100.0
T705Black	0.438	0.168	99.4	0.100	0.025	0.007	0.009	0.005	795	4.00	0.778	100.2
T705Red	1.190	0.150	98.8	0.069	0.020	0.005	0.006	0.003	1110	3.45	0.833	100.3
T705Blue	1.068	0.151	98.5	0.069	0.020	0.005	0.006	0.003	1107	3.45	0.833	99.9

3.2 LASER RAMAN SPECTROSCOPY

In 2004, DORISS acquired *in situ* spectra from the active methane plumes at Hydrate Ridge, sampling the same two sites that were sampled for gas chromatography. The resulting spectra are nearly identical and are displayed in Figure 7.
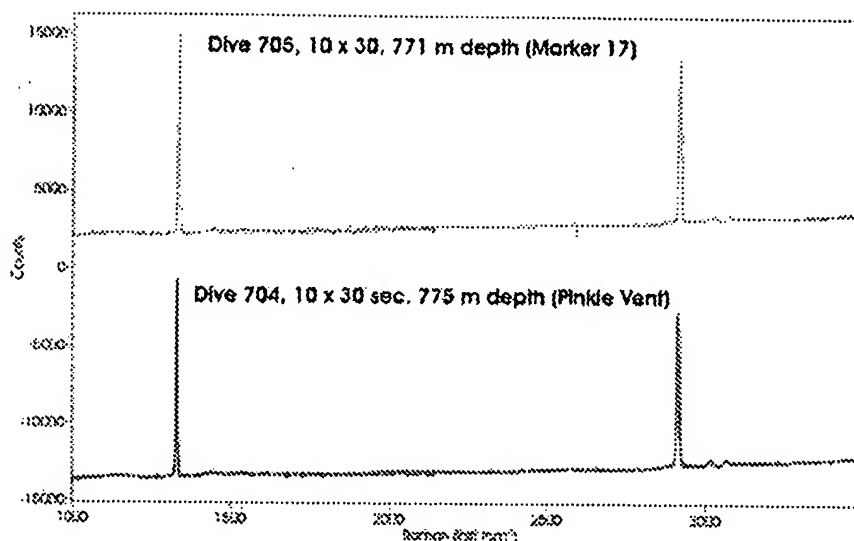
Figure 7: Raman spectra obtained from free gas collected at two different venting sites at Hydrate Ridge.

The diamond in the apparatus shows a peak at 1332cm^{-1}. The large peak at 2915cm^{-1} and smaller peaks at 3020cm^{-1} & 3070cm^{-1} are indicative of methane. The spectrum can be further analyzed with magnification of spectra containing the methane peaks. Figure 8 illustrates the peaks resulting from the v_1, v_2, and $2v_2$ stretching modes of the methane molecule, along with the smaller peaks caused by coupled rotational-vibrational motion. No spectra associated with different gases were detected, which is consistent with the gas chromatographic analysis that methane is the main component in the free gas.
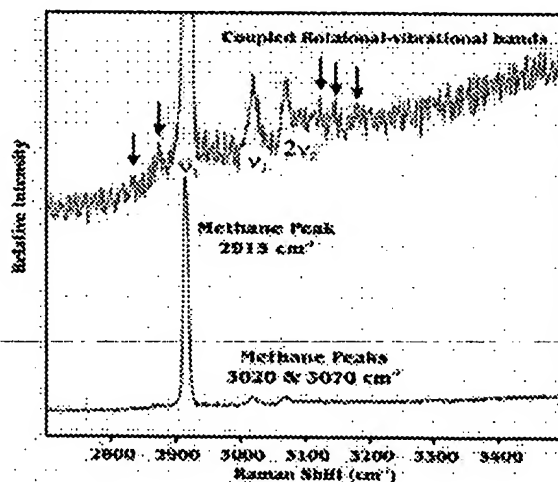
Figure 7: Amplified Raman spectrum collected at Hydrate Ridge.

9

4. DISCUSSION

The $\dfrac{C_1}{C_2 + C_3}$ ratio was high at all venting sites, indicating that the methane at Hydrate Ridge is predominantly biogenically derived from bacterial methanogensis (Dillon & Max, 2000). However, the presence of higher hydrocarbons ($C_2 \rightarrow$ i-C_5) in our gas samples provides evidence that some of the methane is thermogenically produced through geologic processes. From the presence of C_4 and i-C_4 in the free gas samples, it can be inferred that Structure II must be present in the hydrate matrix. However, the high concentration of C1, C_2 and C_3 hydrocarbons, with respect to C_4 and i-C_4 hydrocarbons, indicates that Structure I is the dominant form over Structure II. Of interest is the general absence of n-pentane, while i-pentane is present in trace amounts. This is consistent with the presence of a small proportion of Structure H hydrate, which excludes n-pentane, but can incorporate i-pentane as the guest gas molecule. Thus, the hydrate composition at Hydrate Ridge is dominated by Structure I, with minor amounts of Structure II hydrate and trace quantities of Structure H hydrate.

The Raman spectra clearly detected that the gas was predominantly comprised of methane. However, DORISS was unable to discern the hydrocarbons present in much smaller concentrations (<2%). This is most likely due to the precision of the DORISS apparatus, and this should be taken into account when analyzing *in situ* samples.

Another significant finding is the absence of H_2S in the free gas. This finding supports the kinetic mechanism hypothesis for free gas existence in the hydrate stability zone (Suess et al., 1999). The theory proposed by Milkov et al. (2000), in which there is a creation of a gas hydrate, free gas, and brine equilibrium, must assume equilibrium of all gases in the system. As sediment samples collected from this region are rich in H_2S (data not shown), this hypothesis cannot explain the absence of H_2S in the free gas plume. It could then be proposed that n-pentane might exist in tiny amounts in equilibrium in the sediment matrix as well. Conversely, the kinetic mechanism of isolating the free gas from the sediment matrix through the formation of a hydrate membrane would be consistent with the results presented here.

5. CONCLUSIONS/RECOMMENDATIONS

Hydrate Ridge has a mixed hydrate formed from Structures I, II, and H hydrates. Methane gas is the main component of the free gas vents from and is primarily of biogenic origin, but carbon isotope analysis is needed to confirm this finding. A small amount of the natural gas contained in the system is of thermogenic origin, as indicated by the higher hydrocarbons. The free gas exists within the gas hydrate stability zone inside a hydrate shell creating reservoirs beneath the sediment surface, and is isolated from surrounding pore waters and gases. Better detection of H_2S in the free gas samples is needed to make firm conclusions concerning the mechanism for free gas stability, as well as testing the sediment pore water for n-pentane. This study also shows that laser Raman spectroscopy is a valuable tool able to determine the identity of the major component in free gas *in situ* at an oceanic clathrate. It would be very beneficial, though, to design laser Raman spectroscopy system for the deep-ocean that is more precise and able to detect gases in much lower concentrations.

ACKNOWLEDGEMENTS

References:

Tryon, M.D., K.M. Brown, M.E. Torres (2002). Fluid and chemical flux in and out of sediments hosting methane hydrate deposits on Hydrate Ridge, OR, II: Hydrological processes. *Earth and Planetary Science Letters*, 201: 541-557.

Dickens, G.R., J.R. O'Neil, D.K. Rea, R.M. Owen (1995). Dissociation of oceanic methane hydrate as a cause of the carbon isotope excursion at the end of the Paleocene. *Paleoceanography*, 10: 965-971.

Kvenvolden, K.A. (1988). Methane hydrate- a major reservoir of carbon in the shallow geosphere? *Chemical Geology*, 71: 41-51.

Paull, C.K., W.J. Buelow, W. Ussler, W.S. Borowski (1996). Increased continental-margin slumping frequency during sea-level lowstands above gas hydrate-bearing sediments. *Geology*, 24: 143-146.

Heeschen, K., A.M. Trehu, R.W. Collier, E. Suess, G. Rehder (2003). Distribution and height of methane bubble plumes on the Cascadia Margin characterized by acoustic imaging. *Geophysical Research Letters*, 30: 1-4.

MacKay, M.E., et al. (1992). Landward vergence and oblique structural trends in the Oregon margin accretionary prism: Implications and effect on fluid flow. *Earth and Planetary Science Letters*, 109: 447-491.

Torres, M.E., J. McManus, D.E. Hammond, M.A. de Angelis, K.U. Heeschen, S.L. Colbert, M.D. Tyron, K.M. Brown, E. Suess (2002). Fluid and chemical flux in and out of sediments hosting methane hydrate deposits on Hydrate Ridge, OR, I: Hydrological provinces. *Earth and Planetary Science Letters*, 201: 525-540.

Milkov, A.V., G.R. Dickens, G.E. Claypool, Y. Lee, W.S. Borowski, M.E. Torres, W. Hu, H. Tomaru, A.M. Trehu, P. Schultheiss (2004). Co-existence of gas hydrate, free gas, and brine within the regional gas hydrate stability zone at Hydrate Ridge (Oregon Margin): evidence from prolonged degassing of a pressurized core. *Earth and Planetary Science Letters*, 222: 829-843.

Suess, E., M.E. Torres, G. Bohrmann, R.W. Collier, J. Greinert, P. Linke, G. Rehder, A. Trehu, K. Wallmann, G. Winckler, E. Zuelger (1999). Gas hydrate destabilization: enhanced dewatering, benthic material turnover and large methane plumes at the Cascadia convergent margin. *Earth and Planetary Science Letters*, 170: 1-15.

Dillon, W.P., M.D. Max. "Oceanic Gas Hydrates," Natural Gas Hydrate in Oceanic and Permafrost Environments. Kluwer Academic Publishers, Boston. p61-76, (2000).

Kvenvolden, K.A. (1993). Gas hydrates – Geological perspective and global change. *Reg. Geophys.*, 31: 173-183.

Sassen, R., H.H. Roberts, R. Carney, A.V. Milkov, D.A. DeFreitas, B. Lanoil, C. Zhang, (2004) Free hydrocarbon gas, gas hydrate, and authigenic minerals in chemosynthetic communities of the northern Gulf of Mexico continental slope: relation to microbial processes. *Chemical Geology*, 205: 195-217.

J. D. Pasteris, B. Wopenka, J. Freeman, P. G. Brewer, S. N. White, E. T. Peltzer, and G. E. Malby (2004) Raman spectroscopy in the deep ocean: successes and challenges, *Appl. Spectrosc.*, 58 (7), 195A-208A.

Brewer, P. G., G. Malby, J. D. Pasteris, S. N. White, E. T. Peltzer, B. Wopenka, J. Freeman, and M. O. Brown (2004) Development of a laser Raman spectrometer for deep-ocean science, *Deep Sea Res. I*, 51: 10.1016/j.dsr.2003.11.005.